13. CRETACEOUS INTERACTIONS BETWEEN VOLCANISM AND SEDIMENTATION IN THE EAST MARIANA BASIN, FROM MINERALOGICAL, MICROMORPHOLOGICAL, AND GEOCHEMICAL INVESTIGATIONS (SITE 585, DEEP SEA DRILLING PROJECT)[1]

Hervé Chamley, Hervé Coulon, Pierre Debrabant, and Thierry Holtzapffel, Sédimentologie et Géochimie, Université de Lille I[2]

ABSTRACT

At Site 585 of Deep Sea Drilling Project Leg 89 more than 500 m of volcaniclastic to argillaceous middle-Late Cretaceous sediments were recovered. Analyses by X-ray diffraction (bulk sediment and clay fraction), transmission electron microscopy, molecular and atomic absorption, and electron microprobe were done on Site 585 samples. We identify four successive stages and interpret them as the expression of environments evolving under successive influences:

Stage 1, late Aptian to early Albian—subaerial and proximal volcanism, chiefly expressed by the presence of augite, analcite, olivine, celadonite, small and well-shaped transparent trioctahedral saponite, Al hydroxides, Na, Fe, Mg, and various trace elements (Mn, Ni, Cr, Co, Pb, V, Zn, Ti).

Stage 2, early to middle Albian—submarine and less proximal volcanic influence, characterized by dioctahedral and hairy Mg-beidellites, a paucity of analcite and pyroxenes, the presence of Mg and K, and local alteration of Mg-smectites to Mg-chlorites.

Stage 3, middle Albian to middle Campanian—early marine diagenesis, marked by the development of recrystallization from fleecy smectites to lathed ones (all of alkaline Si-rich Fe-beidellite types), by the development of opal CT and clinoptilolite, and by proximal to distal volcanic influences (Na parallel to Ti, K). Local events consist of the supply of reworked palygorskite during the Albian-Cenomanian, and the recurrence of proximal volcanic activity during the early Campanian.

Stage 4, late Campanian to Maestrichtian—development of terrigenous supply resulting from the submersion of topographic barriers; this terrigenous supply is associated with minor diagenetic effects and is marked by a clay diversification (beidellite, illite, kaolinite, palygorskite), the rareness of clay recrystallizations, and the disappearance of volcanic markers.

INTRODUCTION

Deep Sea Drilling Project Holes 585 and 585A, drilled during Leg 89 in the Mariana Basin (northwestern tropical Pacific, Fig. 1), permitted the recovery of over 500 m of volcaniclastic to argillaceous middle-Late Cretaceous sediments. Site 585 is located north of Ita Maitai Guyot (13°29.00′N, 156°48.91′E; water depth 6109 m; penetration 763.7 m at Hole 585, 892.8 m at Hole 585A). The sedimentary section at this site is divided into six lithologic units (Moberly, Schlanger et al., 1983, and this volume): I—nannofossil ooze and brown clay (Pleistocene, 0–7 m,); washing followed recovery of Unit I to Unit II; II—nannofossil chalk, siliceous limestone, chert, zeolitic claystone (middle Eocene-Maestrichtian, 256–399 m); III—zeolitic claystone with nannofossils, chalk, and chert (Maestrichtian-late Campanian, 399–426 m); IV—chert and zeolitic claystone (Campanian, 426–485 m); V—claystone, locally with zeolites, graded radiolarian fine sand, organic-rich laminae, and carbonate (Campanian-middle Albian, 485–590 m); VI—volcanogenic sandstones, mudstones, and breccias with shallow-water debris (middle Albian-late Aptian, 590–892.8 m).

Our objective was to describe and interpret the conditions of Cretaceous sedimentation in the Mariana Basin

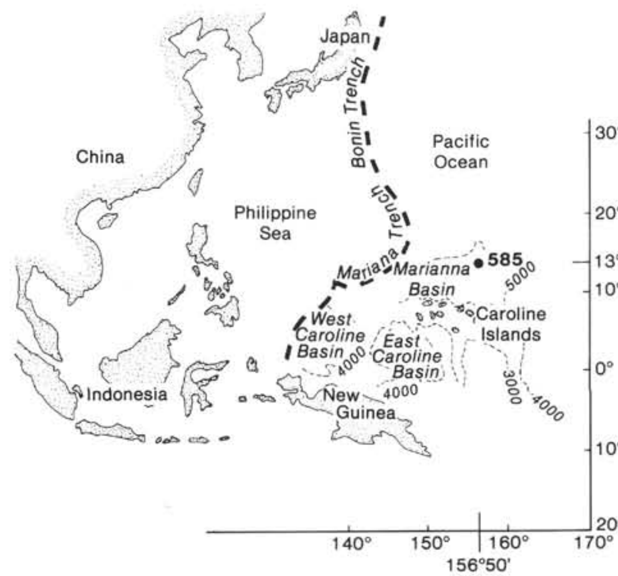

Figure 1. Location of Site 585, DSDP Leg 89.

from mineralogical, micromorphological, and geochemical investigations of Site 585 materials. Fifty samples from the Aptian to Maestrichtian section were analyzed using X-ray diffraction (bulk material and clay fraction) and molecular and atomic absorption (bulk material); 21 samples were studied by transmission electron microscopy on particles smaller than 4 or 2 μm. The techniques used in these analyses are those described by Chamley et

[1] Moberly, R., Schlanger, S. O., et al., *Init. Repts. DSDP*, 89: Washington (U.S. Govt. Printing Office).

[2] Address: Sédimentologie et Géochimie, ERA 764, Université de Lille I, 59655 Villeneuve d'Ascq Cedex France.

al. (1983) and Chamley and Debrabant (1984). Additional geochemical data on clay minerals were provided by studying the [060] peaks on X-ray diffraction diagrams of nonoriented powders, using the methods summarized by Desprairies (1983b).

Microchemical analyses of the clay fraction (<2 μm) of six samples (585-27-1, 13–15 cm; 585-31-3, 29–31 cm; 585-44-3, 17–19 cm; 585-46-2, 40–42 cm; 585-48-2, 4–6 cm; and 585A-17-1, 15–17 cm) were made using a CAMEBAX electron microprobe apparatus, consisting of three spectrometers working simultaneously and automatically. The following elements were measured semiquantitatively: Na, Si, Al (reference to albite), Fe, Ca (reference to andradite), K (reference to orthoclase), Mg, Ti, Mn, Cr, Ni, Zn (reference to different pure substances). The results are expressed in mass concentrations of oxides and reported in weight percentages after correction of the absorption and fluorescence effects.

We present the mineralogy, micromorphological, and geochemical results before discussing the data in terms of evolutionary environments. As the changes recorded from the different technical approaches are generally synchronous, we use the same stratigraphic zonation for each method (Table 1). Four zones are identified and considered in stratigraphic order.

MINERALOGY

The main clay mineralogical results, combined with general lithologic and geochemical data, are presented in Figure 2. Semiquantitative data of the bulk mineralogy are summarized in Table 2.

Zone 1 comprises the lower part of lithologic volcaniclastic Unit VI (Cores 585-55 to -48, and Cores 585A-19 to -11, 892.8–686.1 m); the bulk mineralogy of this zone (late Aptian–early Albian) is characterized by the occurrence of abundant analcite, fairly abundant celadonite, titaniferous augite, and clay minerals. The absence of quartz and the occasional presence of common olivine and of rare feldspars typically characterize this mineralogical zone. Calcite is absent or very rare. The clay mineralogy (less than 2 μm noncalcareous particles) shows highly variable assemblages dominated either by smectite or by smectite and a micaceous mineral. Highly crystallized smectite is the exclusive mineral occurring in the clay fraction of the lowermost volcaniclastic sediments of Site 585 (Cores 585A-17 to -19), consisting of various graded sandstones to unorganized breccias, with abundant ooids, benthic foraminifers, rudist fragments, and other shallow-water carbonate debris. In overlying Cores 585A-16 to -11 and Cores 585-55 to -49, well-crystallized smectite (35–85% of the clay fraction, except in Core 49 where smectite is exclusive) is mainly accompanied by variable amounts of a glauconitic mineral, determined by detailed X-ray analyses as typical celadonite (5–55%). Associated minerals include ordinary chlorite (0–10%), irregular mixed layers of illite–smectite, chlorite–smectite, and rarely illite–vermiculite types, and rare feldspars.

Table 1. Stratigraphic zonation used in this chapter.

Mineralogical, micromorphological, (age range) and geochemical zones	Hole 585 cores	Hole 585A cores
4 (late Campanian to Paleocene)	20 to 17	—
3 (middle Albian to middle Campanian)	39 to 26	10 to 5
2 (early to middle Albian)	47 to 43	—
1 (late Aptian to early Albian)	55 to 48	19 to 11

Zone 2. This mineralogical zone (Cores 585-47 to -43, 686.1–636.1 m) corresponds to the upper part of lithologic Unit VI (Cores 585-42 to -40 have not been studied). The mineralogy of this early to middle Albian series is little different from that determined in the lower part of Unit VI (Zone 1), which corresponds to the continuing volcaniclastic character of the sedimentation.

The main differences in the bulk mineralogy consist of the appearance of rare quartz and true illite, the moderate augmentation of feldspars, the great increase in the abundance of clay minerals, the ubiquity of calcite in small amounts, and the disappearance of olivine. Analcite and augite remain present in significant amounts, and decrease in concentration upsection. The clay mineralogy shows the occasional occurrence of poorly crystallized chlorite associated with expandable layers and some chlorite–smectite irregular mixed layers (585-46-2, 40–42 cm especially), as well as traces of kaolinite (585-45-1, 8–10 cm) and of rare but rather ubiquitous quartz and feldspars. The uppermost part of the zone (from Core 585-45 upward) is characterized by the disappearance of chlorite and irregular mixed layers, and the strong augmentation of highly crystallized smectite, which becomes nearly exclusive in Cores 585-44 and -43.

Zone 3. The third mineralogical zone (middle Albian–middle Campanian) extends from Cores 585-39 to -26 and 585A-10 to -5 in the uppermost part of lithologic Unit VI as well as to Units V and IV (636.1–476.3 m). This interval is characterized by the ubiquity of argillites (i.e., claystones). The argillites are often laminated and graded in the lower part (distal turbidites, with radiolarians and carbonates), associated with radiolarians, carbonates, zeolites, or organic matter in the middle part, and rich in zeolites and cherts in the upper part (Fig. 2). A break in the bulk mineralogy (Table 2) separates this mineralogical zone from the underlying one. Quartz becomes ubiquitous and sometimes abundant, opal CT is commonly present and generally abundant, clinoptilolite is ubiquitous but low in abundance. The typical volcanogenic minerals such as analcite, celadonite, and titaniferous augite are absent. Clay minerals occur abundantly; feldspars and calcite are present in various levels and amounts. The clay mineralogy (Fig. 2) shows the large abundance (more than 95%) of well-crystallized smectite (of lesser average crystallinity, however, than in Zones 1 and 2), and the minor presence of true illite (less than 5%). Associate minerals in the less than 2-μm fraction include rare to abundant quartz, abundant opal CT, rare to common feldspars, and clinoptilolite. Original levels occur in Cores 37 to 34 of Hole 585, where medium-crystallized palygorskite occurs in significant amounts, accompanied or not by kaolinite, quartz, feldspars, opal, or clinoptilolite. The same mineralogical pattern occurs in Cores 585A-10 to -9, suggesting the use of clay mineralogical assemblages for stratigraphic

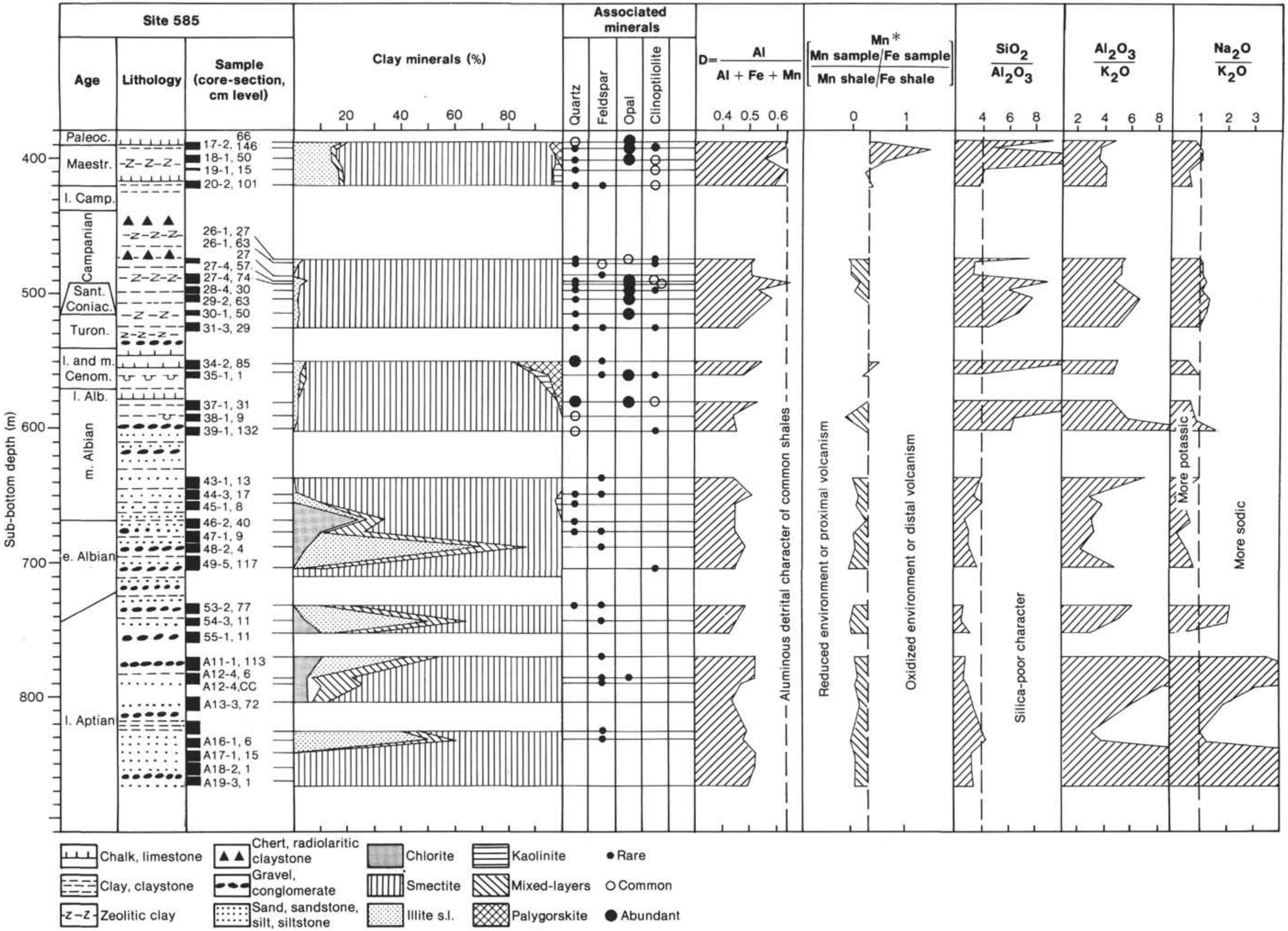

Figure 2. Site 585—main clay mineralogical and geochemical data. (In Sample column, prefix A indicates Hole 585A samples.)

Table 2. Site 585 bulk mineralogy.

Sample (core-section, cm level)	Quartz	Feldspars	Clays	Pyrite	Calcite	Opal CT	Clinoptilolite	Analcite	Celadonite	Augite	Olivine
Hole 585											
17-2, 146	VR	—	AR	—	VA	R	VR	—	—	—	—
18-1, 50	VR	VR	R	—	VA	VA	VR	—	—	—	—
19-1, 15	A	—	A	R	—	—	AR	—	—	—	—
20-2, 101	AR	—	A	R	—	—	AR	—	—	—	—
26-1, 26	R	—	A	—	—	VA	R	—	—	—	—
26-1, 63	—	A	A	—	—	—	R	—	—	—	—
27-1, 13	—	A	A	—	—	—	VR	—	—	—	—
27-4, 57	R	R	AR	—	—	VA	AR	—	—	—	—
27-4, 74	R	—	AR	—	—	VA	AR	—	—	—	—
28-4, 30	AR	—	A	—	R	A	R	—	—	—	—
29-2, 63	AR	R	A	—	VR	A	VR	—	—	—	—
30-1, 50	AR	—	A	—	AR	A	VR	—	—	—	—
31-3, 29	AR	R	VA	—	R	—	R	—	—	—	—
34-2, 85	VA	—	AR	—	AR	—	—	—	—	—	—
35-1, 1	AR	R	A	—	AR	R	—	—	—	—	—
37-1, 31	VA	—	R	—	—	A	—	—	—	—	—
38-1, 9	A	AR	A	—	—	—	—	—	—	—	—
39-1, 132	A	VR	VA	—	R	—	R	—	—	—	—
43-1, 13	VR	R	VA	—	R	—	—	—	—	R	—
44-3, 17	R	AR	A	—	R	—	—	—	—	AR	—
45-1, 8	R	R	VA	—	R	—	—	—	—	—	—
46-2, 40	R	AR	A	—	AR	—	—	AR	—	AR	—
48-2, 4	R	AR	AR	—	AR	—	—	A	AR	AR	—
49-5, 117	—	AR	A	—	—	—	R	—	—	AR	—
54-3, 11	—	—	AR	—	R	—	—	A	AR	R	AR
55-1, 11	—	—	AR	—	—	—	—	—	AR	R	—
Hole 585A											
5-1, 79	VR	R	AR	—	—	VA	VR	—	—	—	—
5-3, 13	AR	R	A	—	R	A	VR	—	—	—	—
7-1, 92	AR	R	A	—	—	R	—	—	—	—	—
7-3, 70	A	R	A	—	—	AR	R	—	—	—	—
8-1, 7	—	A	A	—	—	R	R	—	—	—	—
9-1, 67	A	AR	AR	—	R	A	—	—	—	—	—
10-1, 1	VA	VR	AR	—	R	—	—	—	—	—	—
11-1, 113	—	—	R	—	—	—	—	A	R	AR	—
12-4, 61	—	—	AR	—	—	—	—	A	R	AR	AR
12,CC	—	—	AR	—	—	—	—	A	AR	A	—
15-5, 137	—	R	R	—	R	—	—	A	—	AR	—
16-1, 6	—	R	AR	—	—	—	—	A	AR	AR	—
17-1, 15	—	R	A	—	R	—	—	A	R	R	—
18-2, 1	—	R	A	—	—	—	—	A	R	AR	—

Note: The abundance of each mineral is given by the height of the major peak (I 100) above the background of the powder X-ray diffraction diagrams, according to a conventional scale: very abundant (VA = >150 mm), abundant (A = 40–150 mm), common (AR = 10–40 mm), rare (R = 4–10 mm), very rare (VR = <4 mm) (half values in mm for the poorly crystallized minerals); — = mineral is absent.

correlations. Core 585-34 (20% palygorskite in the clay fraction) corresponds particularly to Core 585A-10 (20% palygorskite), which fits very well with the Cenomanian age given by the biostratigraphy (Premoli Silva and Sliter, this volume). Mineralogical correspondences between both holes in late Albian to Coniacian–Santonian samples are presented in Table 3. Note that the uppermost part of mineralogical Zone 3 (especially Samples 585-27-1, 13–15 cm and 585-26-1, 63–65 cm) shows a few characters evoking some aspects of Zones 1 or 2 (Fig. 2): smectite nearly exclusive and very well crystallized, and the absence of quartz and opal.

Zone 4. The last mineralogical zone occurring in the Cretaceous section (late Campanian, Maestrichtian) corresponds to lithologic Unit III (zeolitic and nannofossil claystone) and overlaps the base of Unit II (chalk). Only sampled in Cores 585-20 to -17, the sediments are characterized by a mineralogical diversification, especially in the clay fraction. Still dominant, smectite is fairly well crystallized and associated with illite (15–20% of the clay fraction), chlorite-smectite irregular mixed layers (traces), kaolinite (0–5%), palygorskite (0–5%), rare quartz, common to abundant clinoptilolite, rare feldspars, and abundant opal CT. The bulk mineralogy shows abundant clay minerals and variable amounts of quartz and clinoptilolite, and the local presence of feldspars, pyrite, calcite, and opal.

MICROMORPHOLOGY

Clay Morphological Types

Transmission electron microscope investigations of the less than 4- or 2-μm fractions from Holes 585 and 585A samples show the presence of many morphological types of clay particles. The most characteristic are the following (Fig. 3; Plates 1–3).

Table 3. Clay mineralogical correspondences in Cores 585-35 to -28 and 585A-10 to -5.

Sample (hole-core-section, cm level)	Illite	Mixed layers	Smectite	Kaolinite	Palygorskite	Quartz	Feldspars	Opal CT	Clinoptilolite
585-28-4, 30	traces	—	100	—	—	+	—	+ + +	+
585-29-2, 63	traces	—	100	—	—	+	—	+ + + +	—
585A-5-1, 79	traces	—	100	—	—	+	—	+ + + +	—
585A-5-3, 13	—	—	100	—	—	+	—	+ + +	+
585-30-1, 50	traces	—	100	—	—	+	—	+ + +	—
585-31-3, 29	traces	—	100	—	—	+	+	—	+
585A-7-1, 92	5	—	95	—	—	+ +	—	+	+ +
585A-7-3, 70	traces	—	100	—	—	+ +	—	+ +	+
585A-8-1, 7	traces	—	100	—	—	—	+ + +	—	+ +
585A-9-1, 67	5	—	95	—	traces	+	—	+ + + +	—
585-34-2, 85	5	—	75	—	20	+ + +	+	—	—
585A-10-1, 1	5	5	70	—	20	+ + +	+	—	—
585-35-1, 1	traces	traces	90	5	5	—	+	+ + +	+

+ = rare; + + = common; + + + = abundant; + + + + = very abundant; — = absent.

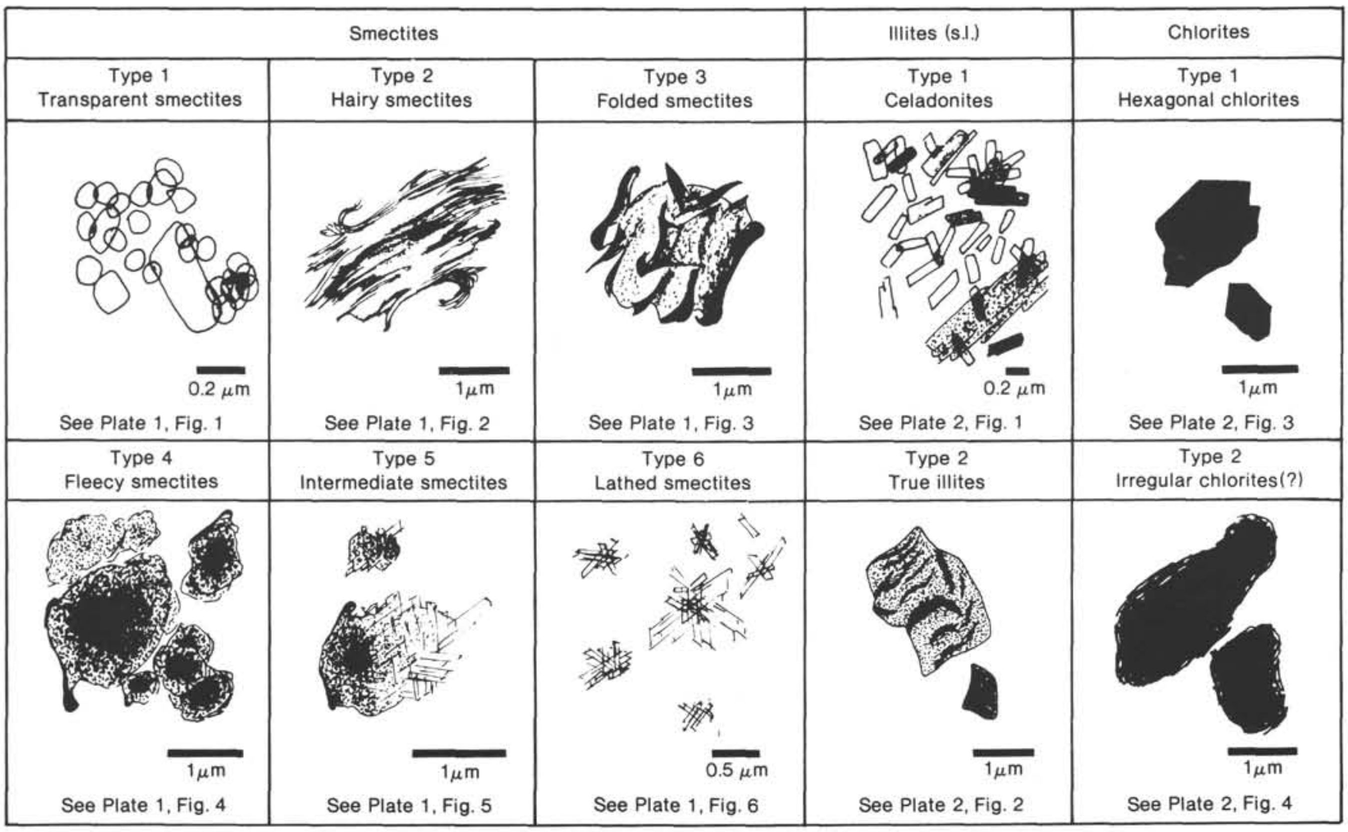

Figure 3. Main clay micromorphological types.

Smectites

Type 1, transparent smectites. These are very small sheets with well-defined but nonpolygonal outlines, nearly transparent to the penetration of electrons. They appear homogeneous, and locally constitute aggregates of larger size (about 2 μm).

Type 2, hairy smectites. These appear as finely folded layers, giving to the particle a hairy shape.

Type 3, folded smectites. This type of clay particle appears in large and flat layers, more or less folded, rather similar to the "opaque smectites" described by Hoffert (1980).

Type 4, fleecy smectites. These are poorly defined sheets with cloudy outlines, sometimes slightly folded, showing various sizes, and commonly described in many Atlantic and Pacific Mesozoic to Cenozoic sediments (e.g., Chamley, 1981; Chamley et al., 1983).

Type 5, intermediate smectites. These resemble fleecy Type 4 smectites, with some outlines consisting of Type 6 lathed sheets.

Type 6, lathed smectites. This assemblage is made up of small and thin lathed sheets at 60° or 120°.

All intermediate stages exist between pure fleecy and pure lathed smectites. This continuous series of particles is very similar to the morphological series described in Albian–Aptian and Paleogene sediments of the North Atlantic Ocean by Holtzapffel et al. (1985); it is interpreted as the result of an early diagenetic evolution from fleecy to lathed smectites.

Micaceous Clays—Illites (s.l.)

Type 1, celadonites. These are very small and slightly elongated chips (0.2–0.5 μm), rather transparent on micrographs when isolated, with well-shaped outlines. They commonly constitute aggregates of larger size.

Type 2, true illites. These are typical micalike sheets, with well-defined and nonpolygonal outlines, fairly large size, and commonly with a watered-looking surface (e.g., Beutelspacher and Van der Marel, 1968).

Chlorites

Type 1, hexagonal chlorites. These form large dark sheets with hexagonal to pseudohexagonal outlines, suggesting an ordered growth.

Type 2, irregular chlorites(?). These are large dark sheets with poorly defined shape (often sharp but nonpolygonal and irregular outlines, locally finely folded sheets, locally transitional shape with cloudy structures).

Palygorskite

These clay particles take the form of typical elongated fibers, forming bundles, or isolated and more or less broken particles.

Kaolinite

Typical hexagonal, isolated, and fairly small sheets characterize this type of particle.

Stratigraphic Distribution

The four zones identified from the mineralogical data show specific micromorphological features.

Zone 1. From Cores 585-55 to -48 and from Cores 585A-19 to -11, this volcaniclastic assemblage is characterized by the presence of transparent smectites (Type 1) and celadonite chips (Plate 2, Fig. 1). Their abundance, estimated by counting on micrographs, corresponds to the relative abundance of each mineral deduced from X-ray diffraction analyses (Fig. 2). Fleecy smectites (Type 4) locally occur in very low amounts. Small quantities of hexagonal chlorite are recognized at some levels (585-54-3, 11 cm; 585-48-2, 4 cm) (Plate 3, Fig. 1). At the base of the zone (585A-15-5, 137 cm; 585A-17-1, 15 cm) small dark particles with with spiral shape occur, constituting in some cases large aggregates (about 2 μm) (Plate 2, Fig. 6). The shape of these particles resembles Fe or Al oxides (Beutelspacher and Van der Marel, 1968).

Zone 2. Ranging from Cores 585-47 to -43), this zone strongly differs from the underlying one. Transparent smectite (Type 1) and celadonite are still present in very small amounts at the base of the zone (e.g., Sample 585-47-1, 9 cm) but disappear upwards. The main differences consist of the appearance of fleecy, intermediate, and lathed smectites (Types 4, 5, 6) showing highly variable relative abundances (e.g., fleecy smectites predominate in 585-44-3, 17 cm; Plate 3, Fig. 4). In some cases (Cores 585-44 and -45), hairy smectites (Type 2) occur in low amounts (Plate 1, Fig. 3). Micaceous clay particles, poorly represented in this zone, generally consist of true illite.

Zone 3. Between Cores 585-39 and -26 and Cores 585A-10 and -5, fleecy, intermediate, and lathed smectites (Types 4, 5, 6) are still present, but the fleecy type is always predominant (Plate 3, Fig. 3). True illite occurs in small quantities. Two peculiar levels, also recognized by X-ray mineralogy, exist in this zone. The first level (585-34-2, 85 cm and 585A-10-1, 1 cm) corresponds to the presence of palygorskite, characterized by numerous independent to bundled fibers associated with fleecy to lathed smectites (Plate 2, Fig. 5). The second level (585-27-1, 13 cm to 585-26-1, 63 cm), particularly well characterized by micromorphology, is located in the uppermost part of Zone 3 and shows the presence of easily recognizable folded smectites (Type 3) in significant amounts (Plate 3, Fig. 5). This type of smectite does not occur below (e.g., 585-27-4, 57 cm); it seems to appear suddenly but to disappear progressively at the top of Zone 3 (585-26-1, 27 cm).

Zone 4. From Cores 585-20 to -17), the mineralogical diversification identified by X-ray diffraction (smectite, illite, palygorskite, and/or kaolinite, irregular mixed layers) is corroborated by electron microscope data (Plate 3, Fig. 6). The smectite morphology is fairly homogeneous and characterized by the large abundance of the fleecy Type 4. Intermediate and lathed smectites (Types 5 and 6) are very rare, which suggests little or no diagenetic effects on clay mineralogy (Holtzapffel and Chamley, 1983).

GEOCHEMISTRY

The geochemical data obtained by molecular and atomic absorption analyses and by microprobe investigations support the distinction of the same four stratigraphic zones previously outlined. The rough geochemical data are given in Tables 4 and 5. Some samples have been subdivided in two or three distinct parts, because of different lithologies (585-26-1, 27 cm; 585-34-2, 85 cm; 585A-10-1, 1 cm). Figure 2 summarizes the main geochemical trends at Site 585 from different ratios defined by Debrabant and Foulon (1979) and Debrabant and Chamley (1982).

Zone 1

From Cores 585-55 to -48, and Cores 585A-19 to -11), the lower part of Site 585 is characterized by the relative abundances of Fe, Mg, and Na (e.g., MgO/Al_2O_3, K_2O/MgO, Na_2O/TiO_2), associated with relatively high amounts of transition trace elements (Mn, Ni, Cr, Co, Pb, V, Ti) and sometimes of Zn. The low and constant values of the SiO_2/Al_2O_3 ratio point to the lack of free

Table 4. Hole 585 geochemical data.

Sample (core-section, interval in cm)	SiO_2 (wt.%)	Al_2O_3 (wt.%)	Fe_2O_3 (wt.%)	CaO (wt.%)	MgO (wt.%)	Na_2O (wt.%)	K_2O (wt.%)	TiO_2 (wt.%)	P_2O_5 (wt.%)	Sr (ppm)	Mn (ppm)	Zn (ppm)	Li (ppm)	Ni (ppm)	Cr (ppm)	Co (ppm)	Cu (ppm)	Pb (ppm)	V (ppm)
1-1, 85-87	48.60	16.13	9.85	2.53	3.45	5.08	2.34	1.04	0.60	268	8337	484	66	336	121	123	382	76	170
17-2, 66-67	76.30	8.25	3.32	1.58	1.80	1.42	1.68	0.34	0.20	116	957	337	34	58	56	14	166	50	20
17-2, 146-148	14.40	2.95	0.96	41.09	0.79	0.80	0.79	0.15	n.d.	679	2562	111	14	40	27	17	41	49	30
18-1, 50-55	47.70	2.68	1.49	22.59	0.67	0.78	0.73	0.19	0.30	452	563	205	11	27	24	6	29	28	10
19-1, 15-17	57.30	13.93	5.92	2.55	3.04	2.08	3.27	0.22	0.50	216	1005	279	66	152	51	38	149	46	60
20-2, 101-104	52.90	13.90	6.96	1.62	2.72	2.50	3.39	0.22	1.90	347	1473	179	42	158	67	39	183	48	50
26-1, 27-29W	69.70	7.62	4.68	1.52	1.99	1.55	1.36	0.81	0.40	184	389	116	21	65	124	19	48	49	80
26-1, 27-29B	60.20	10.16	7.95	2.31	2.95	1.87	1.81	1.00	0.60	221	626	216	36	105	122	30	67	34	60
26-1, 63-65	51.40	14.67	10.74	3.40	2.54	3.16	2.72	1.37	n.d.	358	973	316	20	34	36	17	19	32	50
27-1, 13-19	50.40	14.91	10.61	2.36	2.31	3.20	2.82	1.46	n.d.	358	920	190	17	31	42	13	10	35	60
27-4, 57-60	70.30	7.58	2.70	1.36	1.29	2.07	1.58	1.04	n.d.	237	415	100	10	37	95	5	5	29	70
27-4, 74-76	71.40	8.39	4.02	1.51	1.55	2.03	1.73	0.86	n.d.	237	447	9842	12	37	89	8	11	21	30
28-4, 30-32	61.20	10.35	6.71	3.75	2.67	2.09	1.80	0.92	n.d.	231	679	1904	20	45	43	16	68	26	130
29-2, 63-65	69.30	8.92	4.77	2.28	2.45	1.86	1.34	0.86	n.d.	163	757	2099	17	30	60	14	32	30	70
30-1, 50-52	61.80	8.91	5.98	5.42	2.35	1.88	1.47	0.92	n.d.	216	1173	436	23	42	30	14	27	20	50
31-3, 29-30	53.80	11.19	9.58	3.55	3.53	2.32	2.17	1.13	n.d.	221	1794	166	42	55	65	19	14	35	30
34-2, 85-87W	41.50	3.06	1.95	24.76	0.87	0.44	0.62	0.20	n.d.	337	1326	111	12	28	20	6	14	27	20
34-2, 85-87B	70.50	8.75	5.20	1.70	2.35	0.91	1.70	0.47	n.d.	95	537	121	26	63	54	19	38	64	50
35-1, 1-3	58.20	10.94	8.19	5.52	3.01	2.16	2.29	1.14	0.20	216	1499	121	23	98	43	57	19	36	80
37-1, 31-33	81.60	5.23	3.48	1.44	1.44	0.84	1.09	0.37	n.d.	116	600	105	22	55	50	15	43	24	20
38-1, 9-11	67.90	10.40	10.02	2.48	2.53	1.56	1.75	0.88	0.20	179	747	142	23	55	24	21	12	52	50
39-1, 132-133	61.30	9.64	8.60	4.39	2.52	1.30	0.73	1.44	n.d.	268	1378	126	32	99	149	34	23	16	100
43-1, 13-15	50.10	12.45	11.94	4.42	5.10	1.94	1.76	2.17	0.50	279	1215	189	35	120	123	52	90	33	170
44-3, 17-19	48.50	14.23	10.28	5.30	3.88	1.27	4.68	1.87	0.30	142	1294	121	29	106	104	34	74	23	130
45-1, 8-10	53.30	12.70	11.51	3.70	5.29	1.66	3.13	1.40	0.30	158	1383	132	35	125	117	27	55	45	100
46-2, 40-42	38.50	13.28	12.08	9.68	6.85	2.34	3.11	1.77	0.30	163	2146	153	48	154	155	44	35	38	190
47-1, 9-12	45.40	14.48	12.99	4.13	4.68	1.34	4.26	1.70	n.d.	137	1336	142	40	122	114	32	n.d.	16	60
48-2, 4-8	43.10	13.90	10.89	9.59	3.17	3.84	5.76	1.91	0.30	95	1215	132	15	84	72	28	67	34	120
49-5, 117-119	51.70	13.68	12.71	5.28	3.45	2.50	2.69	2.34	0.30	726	1073	n.d.	26	95	83	47	10	28	140
53-2, 77-78	39.50	14.39	10.55	10.41	3.32	5.05	2.27	1.73	0.20	132	1110	174	14	93	144	24	32	26	130
54-3, 11-13	39.40	15.78	13.92	6.23	2.93	6.16	3.00	2.27	n.d.	84	1288	184	14	74	148	42	37	37	200
55-1, 11-15	45.60	14.05	13.67	5.18	4.62	1.26	4.42	1.67	0.20	137	1341	452	38	107	77	44	16	29	150

Note: B = black and W = white parts of sediment; n.d. = not determined.

Table 5. Hole 585A geochemical data.

Sample (core-section, interval in cm)	SiO_2 (wt.%)	Al_2O_3 (wt.%)	Fe_2O_3 (wt.%)	CaO (wt.%)	MgO (wt.%)	Na_2O (wt.%)	K_2O (wt.%)	TiO_2 (wt.%)	P_2O_5 (wt.%)	Sr (ppm)	Mn (ppm)	Zn (ppm)	Li (ppm)	Ni (ppm)	Cr (ppm)	Co (ppm)	Cu (ppm)	Pb (ppm)	V (ppm)
5-1, 79-80	77.70	5.43	2.53	2.32	1.45	1.53	0.88	0.56	n.d.	132	1278	1265	9	11	33	n.d.	9	18	20
5-3, 13-14	64.90	8.72	4.46	3.03	2.12	1.95	1.50	0.78	n.d.	195	1835	563	17	20	31	7	47	22	50
7-1, 92-94	60.90	10.42	8.71	1.55	3.63	2.00	1.87	1.07	n.d.	179	1535	137	39	87	94	31	36	28	30
7-3, 70-72	61.90	10.04	4.93	2.49	2.70	1.75	1.74	1.06	n.d.	163	5697	168	35	77	67	12	60	30	80
8-1, 7-9	57.30	15.53	7.57	2.10	1.94	3.88	3.24	1.71	n.d.	352	1073	147	11	30	48	16	101	33	80
9-1, 67-71	68.30	5.66	2.48	7.54	1.45	1.51	1.24	0.42	n.d.	152	2078	121	19	35	28	9	39	25	30
10-1, 1-3B	73.90	7.63	4.95	1.37	2.23	1.00	1.81	0.58	0.50	95	631	142	27	78	73	21	67	25	40
10-1, 1-3S	81.90	4.62	3.00	1.19	1.47	0.70	1.20	0.78	0.50	53	479	258	20	52	59	8	40	23	20
10-1, 1-3W	70.20	5.71	3.48	5.44	1.61	0.79	1.47	0.77	1.70	126	831	126	23	75	38	26	42	17	20
11-1, 113-115	45.00	15.63	10.83	6.52	2.92	6.68	1.90	1.96	n.d.	100	1141	163	15	65	79	36	27	41	170
12-4, 61-63	45.30	17.24	11.73	3.85	3.53	7.52	1.15	2.10	n.d.	74	1404	490	20	63	92	35	22	30	200
12,CC	47.30	15.66	13.15	4.60	3.56	5.80	1.85	2.50	n.d.	74	436	205	16	90	151	53	69	30	220
13-3, 72-73	40.30	11.99	11.21	12.13	7.13	3.72	1.92	1.86	n.d.	110	1457	237	29	160	147	49	85	37	180
15-5, 137-139	46.30	11.39	8.81	11.37	2.71	3.70	3.52	1.29	n.d.	1141	842	205	8	98	106	26	60	28	80
16-1, 6-10	46.30	10.98	9.00	11.14	2.77	3.78	2.77	1.29	n.d.	1094	842	142	8	94	113	26	56	29	90
17-1, 15-18	44.30	13.59	9.30	10.05	6.37	6.36	0.25	1.52	n.d.	105	1068	137	7	119	127	35	51	39	150
18-2, 1-3	45.70	13.85	9.38	8.53	6.46	6.48	0.24	1.54	n.d.	126	1073	899	9	130	126	36	50	30	150
19-3, 1-4	45.70	13.45	10.10	8.89	7.91	3.98	0.36	0.88	n.d.	389	1120	3124	20	178	176	42	55	37	16

Note: B = black and W = white parts of sediment; n.d. = not determined.

silica. Potassium is little represented, except toward the top of the zone and seems to be locally associated with Sr (Cores 585A-16 and -17, more than 1000 ppm). P is not detectable until Core 585-55.

The microprobe analysis of 34 particles of Sample 585A-17-1, 15 cm shows the presence of three dominant minerals:

The first of these is *Na-rich magnesian smectite*, which is abundant (70% of the studied particles) and chemically homogeneous (Table 6). The trioctahedral character of the mineral, devoid of Al within the octahedra, and marked by significant amounts of Fe in the tetrahedra and of Na in the interlayers, is corroborated by the [060] X-ray diffraction peak located close to 1.540 Å (Fig. 4). The mineral probably consists of a iron saponite (Millot, 1964), typically generated in volcanic environments (Desprairies, 1981 and 1983a).

The second dominant mineral is *titaniferous augite* with abundant adsorbed Na.

Na_2O (%)	K_2O (%)	CaO (%)	SiO_2 (%)	Al_2O_3 (%)	Fe_2O_3 (%)	MgO (%)	TiO_2 (%)	MnO_2 (%)
11.29	2.33	10.39	38.27	8.97	7.53	12.83	7.80	0.18

The third is *aluminum hydroxide*, not identified by X-ray diffraction, possibly subamorphous, and corresponding to the peculiar spiral particles detected by elec-

Table 6. Microchemical analyses (%) of smectites (average values).

Sample (hole-core-section, cm level)	Age	Na_2O	K_2O	CaO	SiO_2	Al_2O_3	Fe_2O_3	MgO	TiO_2	MnO_2	Types of smectites
585-27-1, 13	Campanian	0.23	1.40	0.92	60.78	15.32	15.47	4.91	0.52	0.25	Fe-beidellites
585-31-3, 29	Turonian	1.87	7.14	0.51	60.03	11.08	12.55	5.53	0.84	0.23	Alkaline smectites
585-44-3, 17	m. Albian	1.09	2.85	1.09	53.24	17.89	11.80	9.19	1.28	0.10	Mg-beidellites
585-46-2, 40	e.–m. Albian	1.40	1.40	0.80	46.93	21.56	9.61	17.69	0.53	0.07	Evolving Mg smectites
585-46-2, 40		1.04	0.86	0.88	43.19	15.41	10.61	27.12	0.69	0.17	(transition to Mg-chlorites)
585A-17-1, 15	Aptian	9.00	3.09	1.68	37.90	10.70	11.83	24.42	0.93	0.20	Saponite

Sample (hole-core-section, cm level)	Zone	Mineralogy	Morphology: Sm. 1	Sm. 2	Sm. 3	Sm. 4–6	Celado.	Chlor. 1	Chlor. 2	X-ray data: d[060] reflection: Results (Å)	Interpretations	Microprobe data
585-26-1, 27	3	Smectites								1.502	Fe or Mg-beidellites	
585-26-1, 63		Smectites								1.502 1.533	Fe or Mg-beidellites (+ saponites?)	
585-27-1, 13		Smectites								1.504 1.533	Fe or Mg-beidellites (+ saponites?)	Only Fe-beidellites
585-27-4, 57		Smectites								1.502	Fe or Mg-beidellites	
585-27-4, 74		Smectites								1.502	Fe or Mg-beidellites	
585-39-1, 132		Smectites								1.502	Fe or Mg-beidellites	
585-44-3, 17	2	Smectites								1.501 1.526	Fe or Mg-beidellites (+ nontronites?)	Only Mg-beidellites
585-44-3, 40		Smectites Chlorites								1.480–1.540	Smectites to chlorite series	Evolving Mg-Sm. to Mg-Chlo.
585-47-1, 9		Smectites Chlorites								1.505	Fe or Mg-beidellites	
585A-11-1, 113	1	Celadonites Smectites								1.509–1.538	Celadonite Saponite	
585A-17-1, 15		Smectites								1.502 1.537	Saponite (+ beidellites?)	Saponite

Figure 4. Location of the [060] X-ray reflection of selected samples and relationships with the micromorphological zonation (see text for morphological types). The size of d-spacing values is proportional to the height of the X-ray diffraction corresponding peak. Sm. 1 = smectite of Type 1, and so on.

tron microscopy (Plate 2, Fig. 6). These particles occur in significant amounts (15%) and are associated with abundant Na.

Na_2O (%)	K_2O (%)	CaO (%)	SiO_2 (%)	Al_2O_3 (%)	Fe_2O_3 (%)	MgO (%)	TiO_2 (%)	MnO_2 (%)
12.05	1.70	1.49	2.35	78.94	1.13	1.95	0.80	0.06

Note that feldspars identified in Sample 585-48-2, 4 cm consist of albite and orthoclase types (Table 7).

Zone 2

In Cores 585-47 to -43, the K abundance tends to increase and the Na abundance to decrease (e.g., $Na_2O/K_2O < 1$, Fig. 2), whereas Mg, Ti, Fe, and Mn remain fairly abundant. The increase in concentration of potassium corresponds to relatively high amounts of feldspars in the bulk sediments.

Microchemical analyses were done on two samples, the first of which—Sample 585-46-2, 40 cm (36 particles)—contains the following minerals:

• *Alkaline feldspars* of K, Na, and K–Na types, forming about 35% of the particles identified and corresponding to different minerals from orthoclase to albite (Table 7).

• *Pyroxenes* (15% of particles) more Si- and Mg-rich and less alkaline than in underlying Zone 1 (diopside-hedenbergite types, Deer et al., 1963a).

Na_2O (%)	K_2O (%)	CaO (%)	SiO_2 (%)	Al_2O_3 (%)	Fe_2O_3 (%)	MgO (%)	TiO_2 (%)	MnO_2 (%)
1.11	0.23	11.15	50.09	6.10	4.63	24.23	1.00	0.10

• *Smectitelike minerals* (35%), constituting an inhomogeneous group marked by the abundance of Mg and gradually ranging from an Al–Si type to a Mg-rich type

Table 7. Microchemical analyses (%) of feldspars (average values).

Sample (hole-core-section, cm level)	Age	Na_2O	K_2O	CaO	SiO_2	Al_2O_3	Fe_2O_3	MgO	TiO_2	MnO_2	Types of feldspars
585-27-1, 13	Campanian	6.21	0.90	6.22	55.62	23.88	5.45	1.18	0.32	0.09	Andesine-oligoclase
		4.46	7.94	0.91	62.86	18.97	3.37	0.91	0.29	0.13	Alkaline-feldspar
585-31-3, 29	Turonian	9.01	2.19	2.82	62.11	20.71	2.13	0.87	0.14	0.03	Albite
		5.84	8.59	0.70	61.88	17.77	3.19	1.43	0.31	0.20	Alkaline-feldspar
585-44-3, 17	m. Albian	1.26	11.18	0.25	61.35	22.02	1.64	1.93	0.30	0.06	Orthoclase
585-46-2, 40	e.–m. Albian	8.33	0.93	1.87	62.33	17.43	2.32	6.77	0.13	0.02	Albite
		8.56	6.16	0.67	57.60	21.11	2.21	3.37	0.26	0.02	Alkaline-feldspar
		0.50	10.13	0.21	61.09	21.33	1.93	4.65	0.05	0.05	Orthoclase
585-48-2, 4	e. Albian	11.17	1.60	0.74	61.96	19.20	2.87	0.97	0.50	0.08	Albite
		0.35	13.76	0.44	63.01	16.96	3.69	1.17	0.38	0.08	Orthoclase
585A-17-1, 15	l. Aptian										No feldspars but aluminum hydroxides

(Table 6) (Weaver and Pollard, 1973). The structural formulas can be calculated as exclusive smectites (Table 8), and in this case the magnesium of the Mg-rich type is abundant in both octahedra and interlayers:

$$(\mathrm{Si_{2.80}Al_{1.18}Fe^{3+}_{0.02}})(\mathrm{Mg_{2.19}Fe^{3+}_{0.50}Ti_{0.03}})\mathrm{Mg_{0.44}Na_{0.13}K_{0.07}Ca_{0.06}O_{10}(OH)_2}$$

The Mg-rich type could also be a transition mineral between a Mg-smectite and a Mg-chlorite. Such a Si-depleted intermediate structure suggests a pseudochlorite, partly expandable, consisting of a transitional mixture of beidellite and of a neutral brucitic interlayer (Caillère et al., 1982):

$$\begin{array}{l|l}(\mathrm{Si_{3.57}Al_{0.43}}) & (\mathrm{Al_{1.07}Fe^{3+}_{0.65}Mg_{0.34}Ti_{0.04}})\mathrm{Na_{0.17}K_{0.10}Ca_{0.08}O_{10}(OH)_2} \\ \multicolumn{2}{c}{\mathrm{Mg_3(OH)_6}}\end{array}$$

This second hypothesis appears more likely, because the presence of the Mg-rich mineral corresponds to poorly crystallized chlorite, associated with expandable layers, and to poorly defined 1.48–1.54 Å reflections (X-ray data, Figs. 2 and 4), and to irregular dark sheets identified on electron micrographs (Plate 2, Fig. 4). The accumulation of Mg in the smectite interlayers progressively would permit the growth of a typical magnesian chlorite, also identified in few amounts by microprobe analysis (see below).

• *Magnesian chlorite*, characterized by a very high proportion of Mg and low proportions of Si:

Na_2O (%)	K_2O (%)	CaO (%)	SiO_2 (%)	Al_2O_3 (%)	Fe_2O_3[a] (%)	MgO (%)	TiO_2 (%)	MnO_2 (%)
0.95	0.52	0.61	36.89	16.21	9.76	33.07	1.66	0.24

[a] (FeO = 8.78 %)

The structural formula of this trioctahedric chlorite is of the following type, in which the tetrahedric substitutions are compensated in the brucitic layer and all the Al is located in tetrahedra:

$$\begin{array}{l|l}(\mathrm{Si_{3.16}Al_{0.84}}) & (\mathrm{Mg_2Fe^{2+}_{0.63}Ti_{0.10}})\mathrm{Na_{0.16}K_{0.06}Ca_{0.06}O_{10}(OH)_2} \\ \multicolumn{2}{c}{(\mathrm{Mg_{2.2}Al_{0.80}})\mathrm{(OH)_6}}\end{array}$$

The second Zone 2 sample microchemically analyzed is 585-44-3, 17 cm (35 particles). Most of the clay-sized particles investigated (65%) are homogeneous magnesian and iron-rich smectites, distinct from those of underlying levels because of higher amounts of Fe_2O_3 than

Table 8. Structural formulas of smectites in Holes 585 and 585A (from microprobe analyses).

Sample (age)	Structural formula	Δo[a]	Total Al	Total Mg	Types of smectites
585-27-1, 13 (Campanian)	$(\mathrm{Si_{3.96}Al_{0.04}})(\mathrm{Al_{1.05}Fe^{3+}_{0.52}Mg_{0.47}Ti_{0.02}})\mathrm{K_{0.10}Ca_{0.09}Na_{0.03}O_{10}(OH)_2}$	0.27	1.09	0.47	Fe-beidellites
	$(\mathrm{Si_{3.79}Al_{0.21}})(\mathrm{Al_{0.92}Fe^{3+}_{0.73}Mg_{0.46}Ti_{0.02}})\mathrm{K_{0.11}Ca_{0.06}Na_{0.03}O_{10}(OH)_2}$	0.05	1.13	0.46	
	$(\mathrm{Si_{3.66}Al_{0.34}})(\mathrm{Fe^{3+}_{0.97}Al_{0.71}Mg_{0.44}Ti_{0.02}})\mathrm{K_{0.15}Ca_{0.06}Na_{0.03}Mg_{0.02}O_{10}(OH)_2}$	0	1.28	0.46	
585-31-3, 29 (Turonian)	$Si^{4+} > 4$, smectites with free SiO_2 (Grim and Kulbicki, 1961)				
	$(\mathrm{Si_{3.88}Al_{0.12}})(\mathrm{Al_{0.72}Fe^{3+}_{0.61}Mg_{0.53}Ti_{0.04}})\mathrm{K_{0.59}Na_{0.24}Ca_{0.04}O_{10}(OH)_2}$	0.79	0.84	0.53	Alkaline smectites
	$(\mathrm{Si_{3.68}Al_{0.32}})(\mathrm{Al_{0.62}Fe^{3+}_{0.68}Mg_{0.58}Ti_{0.03}})\mathrm{K_{0.69}Na_{0.31}Ca_{0.07}O_{10}(OH)_2}$	0.82	0.94	0.58	
585-44-3, 17 (m. Albian)	$(\mathrm{Si_{3.42}Al_{0.58}})(\mathrm{Mg_{0.87}Al_{0.78}Fe^{3+}_{0.56}Ti_{0.06}})\mathrm{K_{0.23}Na_{0.15}Ca_{0.09}Mg_{0.01}O_{10}(OH)_2}$	0	1.36	0.88	Mg-beidellites
585-46-2, 40 (e.–m. Albian)	$(\mathrm{Si_{2.98}Al_{1.02}})(\mathrm{Mg_{1.35}Al_{0.60}Fe^{3+}_{0.46}Ti_{0.03}})\mathrm{Mg_{0.32}Na_{0.32}Na_{0.17}K_{0.11}Ca_{0.05}O_{10}(OH)_2}$	0	1.62	1.67	Evolving Mg-smectites transition to Mg-chlorite
	$(\mathrm{Si_{2.80}Al_{1.18}Fe^{3+}_{0.02}})(\mathrm{Mg_{2.19}Fe^{3+}_{0.50}Ti_{0.03}})\mathrm{Mg_{0.44}Na_{0.13}K_{0.07}Ca_{0.06}O_{10}(OH)_2}$	0	1.18	2.63	
585A-17-1, 15 (l. Aptian)	$(\mathrm{Si_{2.66}Al_{0.87}Fe^{3+}_{0.47}})(\mathrm{Mg_{2.52}Fe^{3+}_{0.17}Ti_{0.04}})\mathrm{Na_{1.21}K_{0.27}Ca_{0.12}O_{10}(OH)_2}$	0.25	0.87	2.52	Saponite

[a] Δo = octahedral charge deficit.

MgO, and identified as a mixture of Mg-beidellites (Tables 6 and 8).

The other particles studied in this sample include potassic feldspars (25%) of orthoclase type (Table 7), and common micaceous minerals of the following composition, probably corresponding to the "true illite" identified by X-ray diffraction and electron microscopy (Deer et al., 1983b):

Na_2O (%)	K_2O (%)	CaO (%)	SiO_2 (%)	Al_2O_3 (%)	Fe_2O_3 (%)	MgO (%)	TiO_2 (%)	MnO_2 (%)
2.33	7.61	0.29	52.19	23.69	8.31	4.62	0.83	0.12

Zone 3

This zone ranges from Cores 585-39 to -26, and from Cores 585A-10 to -5. A major break marked by a strong increase of free silica (SiO_2/Al_2O_3, Fig. 2) occurs between Cores 43 and 39 of Hole 585. The relative decrease of metallic elements is determined by the silica augmentation, as shown by the persistence of noticeable amounts of transition elements in the most argillaceous samples. Zone 3 is also characterized by a strong correlation between Na_2O and TiO_2. The correlation factor $r(Na_2O, TiO_2) = 0.96$ and the corresponding regression line are characteristic of the late Albian to Campanian period: $Na_2O = 2.15\ TiO_2$ (Fig. 5).

The lower part of Hole 585 Zone 3 (Cores 38–34) shows an excess of K compared to Na ($Na_2O/K_2O < 1$, Figs. 2 and 5), whereas the upper part (Cores 31–26) shows a reverse trend ($Na_2O/K_2O > 1$). The same geochemical zonation occurs at Hole 585A, and points to good correlations between both holes. For example, Sample 585A-10-1, 1 cm (black) correlates to Sample 585-34-2, 85 cm (black). Cores 585A-9 to -5 strongly resemble Cores 585-31 to -29 in relative abundance of Na_2O compared to K_2O, development of some transition metals (Mn, etc.), and in Cores 585-29 and 585A-5, parallel increase of SiO_2 and Zn (Tables 4 and 5).

The uppermost part of Zone 3 (585-27-1, 13 cm and 585-26-1, 63 cm) is characterized by a small but sudden increase in Fe and Mn, and in a smaller proportion of Na, K, Ti, and locally P. This particular level corresponds to the presence of folded smectites, which are especially abundant (Plate 3, Fig. 5).

Microprobe analyses were done on two samples. In the first sample, 585-31-3, 29 cm (23 particles), most particles identified (80%) correspond to Si-rich alkaline smectites (Tables 6 and 8), fairly rich in iron, and probably ranging from a type-fixing free silica (Grim and Kulbicki, 1961) to a more aluminous type. The octahedral substitutions are abundant, and compensated by alkaline cations. The other particles chiefly consist of Na-K feldspars, often more calcic than in underlying sediments (Table 7). In the second sample, 585-27-1, 13 cm (36 particles), 70% of the particles identified are Si-rich smectites (Table 6), constituting a group characterized by antagonistic contents of Fe and Si [$r(SiO_2, Fe_2O_3) = -0.81$], and by moderate octahedric substitutions. Different structural formulas can be calculated, ranging from a beidellite s.s. to a Fe-beidellite (Table 8). Other minerals are chiefly feldspars, either potassic or calcic (Table 7).

Zone 4

From Cores 585-20 to 17, the latest Cretaceous sediments show a strong increase of aluminum (see index D, detrital index, in Fig. 2), manganese (see index Mn*, Fig. 2), and phosphorus (P_2O_5, Table 4). The variability of the sedimentation is reflected by variable amounts of

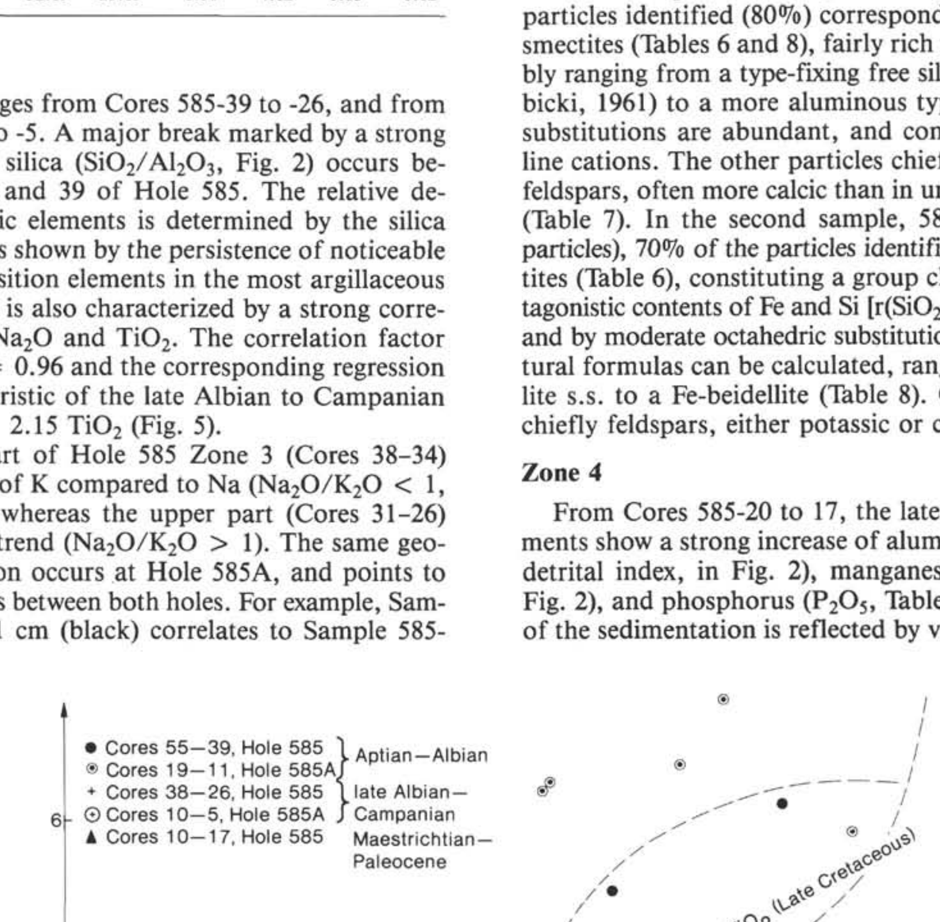

Figure 5. Relationships between Na_2O and TiO_2 at Holes 585 and 585A.

Si and Ca. The mineralogical diversification identified by X-ray diffraction corresponds to common contents of Ti, Fe, and to the predominance of K over Na, frequent in nonvolcanogenic environments (Debrabant and Chamley, 1982).

DISCUSSION AND CONCLUSION

The combined study of mineralogical, micromorphological, geochemical, and microchemical characters of Site 585 sediments, considered in a general lithologic context, gives insight into a paleoenvironmental reconstruction of Mariana Basin history during the Cretaceous (Figs. 6 and 7). Four successive stages are identified.

Stage 1, late Aptian to early Albian Cores 585-55–48; Cores 585A-19–11)

The association of highly crystallized Mg-smectite (Na-saponite), celadonite, analcite, titaniferous augite, olivine, Na- to K-feldspars, and the abundance of Fe, Mg, Na, K, and different trace elements (Mn, Ni, Cr, Co, Pb, V, Zn, Ti) indicate the importance of volcanic influence on the mineralogy and geochemistry of the sediments. This close relationship between inorganic sedimentation and volcanism is corroborated by the lithology, which is characterized by a heterogeneous mixture of volcanic sandstones, mudstones, and breccias (Site 585 report, this volume). As a probable consequence, the small, well-shaped, transparent smectites (apparently not previously described in the literature), the celadonite chips, and the hexagonal chlorites characterize the micromorphology of clay minerals resulting from the evolution of the Site 585 heterogeneous volcanogenic materials. The volcanogenic origin of Cretaceous smectites in Aptian sediments of the Mid-Pacific Mountains has already been suggested by Mélières et al. (1981).

The large amount of numerous volcanogenic particles points to the proximity of Site 585 to volcanoes. Only sparse fleecy smectites could indicate a minor contribution of a more distant supply. The presence of shallow-water calcareous debris (Site 585 report, this volume) suggests the presence of volcanic islands and the subaerial eruption of a large portion of volcanic materials. This interpretation is substantiated by the abundance of Na fixed or adsorbed by most of the minerals; in Mesozoic sediments of the Atlantic sodium has been proposed as a marker of subaerial volcanism (Debrabant and Chamley, 1982). Additional arguments are provided by the presence of aluminum hydroxides of a possible pedogenic origin. Thiede et al. (1982) indicate the importance of terrestrial organic matter in mid-Cretaceous sediments of the tropical and subtropical Pacific Ocean. As a consequence, the transparent and small smectites could be characteristic of alteration products of volcanic materials produced in a Na-rich subaerial environment.

Note that toward the end of Stage 1 (from Cores 585A-16 and -15 upward), the more potassic character of the sediment geochemistry could be related to the abundance of celadonite. Such an interpretation does not fit with the relative abundance of strontium. The association of K and Sr, and locally of P, more likely indicates a change in the geochemical character of volcanism, probably of a trachybasaltic or a trachyandesitic type (Faure, 1978; Stueber, 1978). Feldspar-rich trachytes are described at Site 585 between 850 and 700 m water depth (Site 585 report, this volume). Celadonite could proceed from the alteration of these rocks.

In summary, *Stage 1 at Site 585 indicates the strong influence of a local and subaerial volcanism on the sedimentation.*

Stage 2, early to middle Albian Transition Cores 585-47–43

The bulk and clay minerals continue to include volcanogenic species such as analcite and titaniferous augite, which corresponds to the persistence of the volcanogenic supply shown by lithological observations. The geo-

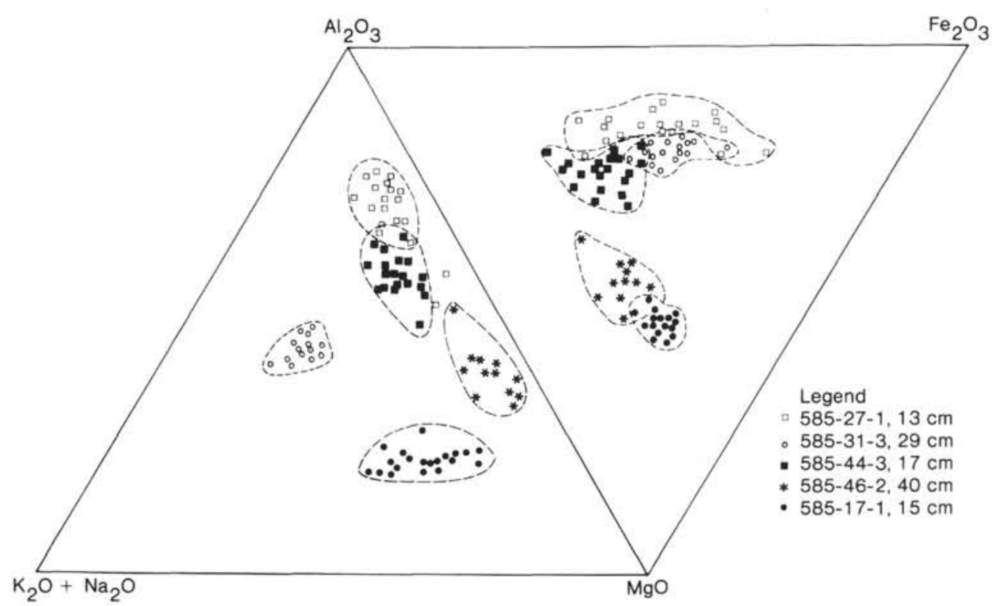

Figure 6. Microchemical correlations of clay minerals from selected samples.

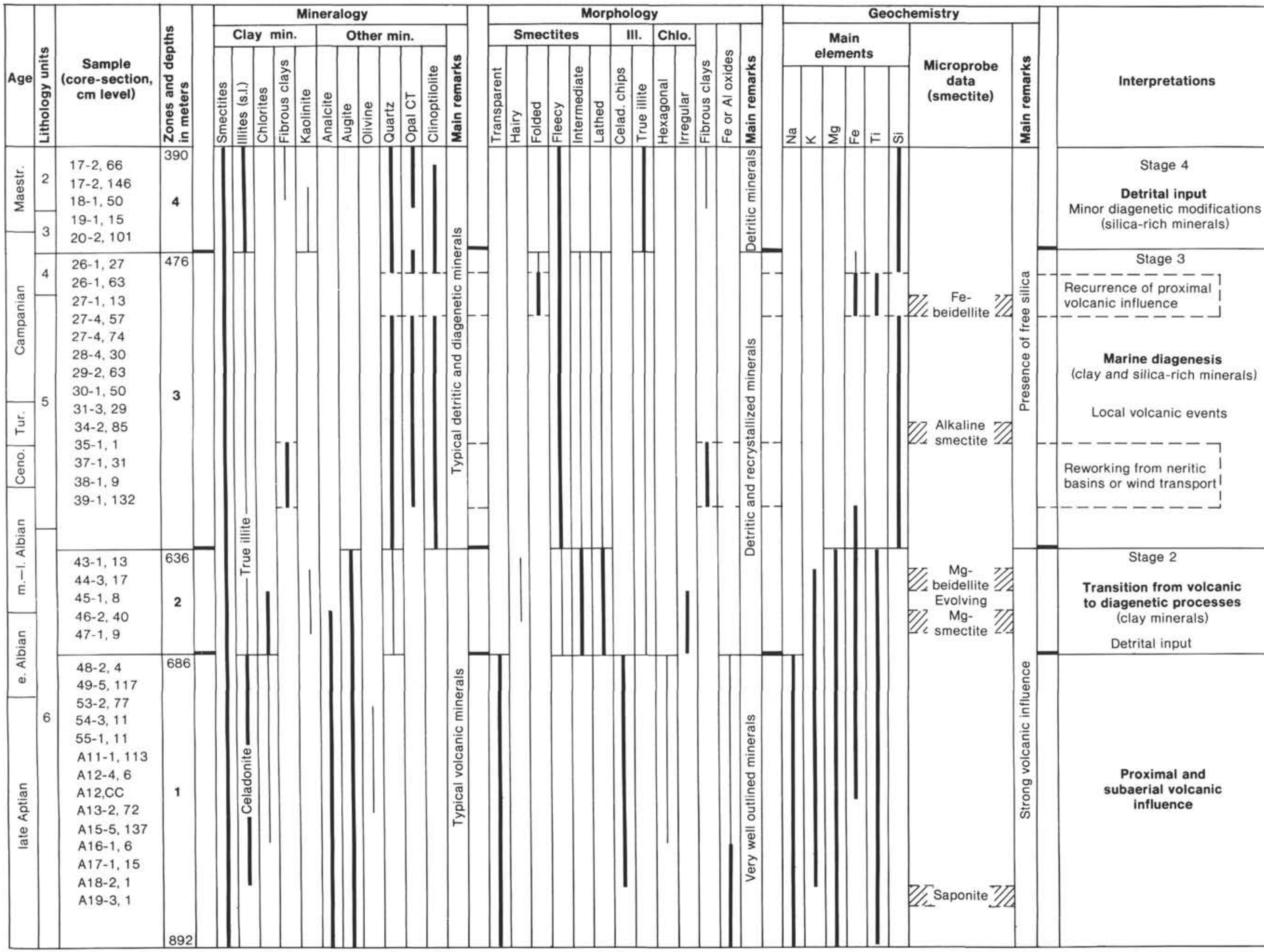

Figure 7. Site 585: main data and interpretations. (In Sample column, prefix A indicates Hole 585A samples.) In Interpretations column, bold-faced lettering indicates major phenomena; minor events are represented by regular lettering.

chemistry confirms the continuing influence of volcanism by the relative abundance of magnesium (Fig. 7), Ti, Fe, and Mn (Table 4); by the parallelism between Na_2O and TiO_2, constant during most of the Late Cretaceous (Fig. 5); and by the abundance of Na- to K-feldspars.

Nevertheless, the volcanic influences appear to be less proximal than during Stage 1, because smectites comprise dioctahedral types with aluminum in the octahedra (Mg-beidellites) (Fig. 6), increased amounts of SiO_2, and decreased amounts of MgO. Volcanogenic micromorphologies, consisting of hairy smectites and of a few transparent smectites (i.e., Stage 1), are largely associated with fleecy to lathed smectites, probably indicative of *in situ* recrystallizations without specific volcanic influence (Holtzapffel et al., 1985). Volcanogenic olivine and celadonite have disappeared, and are superceded by some true illites of a detrital origin. The sodium content decreases, and suggests a lesser contribution of subaerial volcanism. To summarize, *Stage 2, identified by inorganic investigations, appears as a transition period characterized by continuously marked but less proximal and less aerial volcanic influence.*

A singular episode occurred during this stage, especially represented in Core 585-46. A continuous series of clay minerals ranging from Mg-beidellite to Mg-chlorite, including chlorite–smectite irregular mixed layers and expandable chlorite, indicates a change in the depositional conditions, permitting the accumulation of magnesium and the existence of prediagenetic transformations (Millot, 1964). This mineralogical series suggests the *temporary development of a confined environment*, in which the fixation of abundant magnesium on beidellites determined the progressive passage to pseudochloritic and chloritic minerals. Similar diagenetic modifications are believed to have occurred on the northwestern African margin during the lower Mesozoic (Chamley and Debrabant, 1983).

Stage 3, middle Albian to middle Campanian Cores 585-40–26; Cores 585A-10–15

The Stage 2/Stage 3 boundary corresponds to the first strong break recorded in the Site 585 bulk mineralogy, which correlates with the passage of volcanogenic heterogeneous sediments to claystones. The minerals typical of a volcanic influence (augite, analcite) disappear, and are replaced by quartz, opal CT, and clinoptilolite. Smectites associated with minor amounts of true illite remain very abundant, but are commonly not as well crystallized as in volcanogenic deposits and correspond to Si-rich alkaline types (Fig. 6). These data suggest a more distant influence of volcanism, nevertheless still marked by the Na- to K-feldspars and by the Na_2O–TiO_2 correlation (Fig. 5).

The development of opal CT and of clinoptilolite indicates the importance of early diagenetic processes affecting the silica. Other *in situ* changes characterize the smectites, which show a continuous series between fleecy, partly lathed, and completely lathed types. This evolution has been recorded and interpreted in Cretaceous and Paleogene sediments of the North Atlantic (Holtzapffel et al., 1985), and probably corresponds to an *in situ* recrystallization of fleecy smectite to lathed smectite, without significant geochemical or mineralogical quantitative modifications. As a result, *the third period identified during the Cretaceous at Site 585 is characterized by a decrease of volcanic influence and an increase of early diagenetic processes, which chiefly affect silica-rich minerals and smectites of distant origins.*

Two recognizable periods occurred during Stage 3. The first period (Cores 585-37–34, and 585A-10 to -9, late Albian to Cenomanian) is marked by fairly abundant palygorskite and quartz, and by little kaolinite and true illite. *Palygorskite fibers* are quite independent and mixed with other minerals, and do not correspond to any specific lithology. This level could reflect the reworking of neritic basins undergoing a basic chemical sedimentation (Millot, 1964; Weaver and Beck, 1977; Chamley, 1979), perhaps contemporaneous with the tectonic subsidence of volcanic archipelagoes. It could also reflect the supply of distant minerals by wind and marine transport, as recently shown in the Shatsky Rise area during the latest Cretaceous–earliest Paleogene (Lenôtre et al., in press). A third explanation could be the migration of the Mariana Basin across an arid climatic latitudinal zone during the northward movement of the Pacific Plate. Such a reworking points to a diversification of mineralogical sources and perhaps to the diminution of morphological barriers for distant supply.

The second period is evident at the top of Zone 3, in Cores 27 and 26 (Campanian). The local increase of Fe, Mn, Na, K, and Ti as well as the temporary appearance of some folded-smectites, probably of a dioctahedral type (Fe-beidellite) and highly crystallized, suggest a possible *recurrence of a proximal volcanic influence.* Such an event, possibly having occurred elsewhere in the underlying series and not recorded because of sparse recovery (Fig. 2), is also suggested by the Na_2O-K_2O association (Table 4). This association could indicate the presence of Na–Ti amphiboles, well-known in West Pacific trachybasalts or trachyandesites (Aoki, 1959). In spite of that, the sedimentation is marked by a more continental detrital character than in the Aptian–Albian volcanogenic sediments, as shown by its more aluminous and less magnesian chemical composition (Fig. 6, Table 8).

Stage 4, late Campanian to Maestrichtian Cores 585-20–17

The mineralogical diversification occurring during the uppermost Cretaceous (smectite, illite, palygorskite, kaolinite, irregular mixed layers) correlates to a more aluminous character of the geochemistry (D, Fig. 2) and to the strong decrease of clay diagenetic modifications (abundance of fleecy smectites, rarity of partly lathed smectites). These data, together with the strong diminution of volcanogenic markers (Ti, Fe, K, Na), point to the development of the terrestrial detrital character of sedimentation of very distant supply, broadly of pedogenic origin, derived from Asiatic landmasses (e.g., Chamley et al., in press). This major change in environmental conditions probably resulted chiefly from the development of circulation, suggested by the oxidizing precipitation of Mn (Mn*, Fig. 2; Debrabant and Foulon, 1979) and of Ti and Cu, and by the relative abundance of P of biogenic origin. Diagenetic effects persist locally only (opal CT, clinoptilolite), especially in the relatively more permeable carbonate-rich levels. To summarize, *the last Cretaceous stage corresponds to the development of detrital input associated with developing circulation, distant supply, and minor diagenetic modifications.*

To conclude, the mineralogical, micromorphological study of DSDP Site 585 shows that from late Aptian to Maestrichtian a series of sedimentary regimes were successively dominated by volcanogenic, diagenetic, and terrigenous influences. The Mariana Basin first depended on local supply, then progressively received more distant and diversified sedimentary contributions as a result of the submersion of volcanic archipelagoes, the subsidence of submarine barriers, and the development of circulation.

ACKNOWLEDGMENTS

We gratefully acknowledge the U.S. National Science Foundation, the shipboard party of DSDP Leg 89, and especially S. O. Schlanger, M. Baltuck, and A. Schaaf for enabling us to work with Site 585 cores. M. Bocquet, J. Carpentier, J.-C. Deremaux, F. Dujardin, A. Le Maguer, and P. Récourt provided very efficient technical assistance. Very pertinent and useful scientific comments were made by M. Baltuck, A. Desprairies, E. Suess, and J. Schoonmaker. Financial support was provided by A. T. P. 1983 "Géologie et Géophysique des Océans" of C.N.R.S. (France).

REFERENCES

Aoki, K., 1959. Petrology of alkali rocks of the Iki Island and Higashi-Matsuura district, Japan. *Sci. Rept. Tohoki Univ.*, Ser. 3, 3: 261.

Beutelspacher, M., and Van der Marel, M. W., 1968. *Atlas of Electron Microscopy of Clay Minerals and Their Admixtures:* Amsterdam (Elsevier).

Caillère, S., Henin, S., and Rautureau, M., 1982. *Minéralogie des Argiles: Classification des Argiles*, (Vol. II): Paris (Masson).

Chamley, H., 1979. North Atlantic clay sedimentation and paleoenvironment since the Late Jurassic. *In* Talwani, M., Hay, W., and Ryan, W. B. F. (Eds.), *Deep Drilling Research in the Atlantic Ocean: Continental Margins and Paleoenvironment.* Maurice Ewing Ser., Am. Geophys. Union, 3:342-361.

________, 1981. Clay sedimentation and paleoenvironment in the Shikoku Basin since the middle Miocene (Deep Sea Drilling Project Leg 58, North Philippine Sea). *In* Klein, G. deV., Kobayashi, K., et al., *Init. Repts. DSDP*, 58: Washington (U.S. Govt. Printing Office), 669-681.

Chamley, H., Cadet, J.-P., and Charvet, J., in press. Nankai Trough and Japan Trench late Cenozoic paleoenvironments deduced from clay mineralogical data. *In* Kagami, H., Karig, D. E., Coulbourn, W. T., et al., *Init. Repts. DSDP*, 87: Washington (U.S. Govt. Printing Office).

Chamley, H., and Debrabant, P., 1983. Héritage de minéraux métamorphiques et diagenèse dans le Mésozoïque inférieur de la marge Atlantique du Maroc. *C. R. Acad. Sci.*, 296:651-656.

________, 1984. Mineralogical and geochemical investigations of sediments on the Mazagan Plateau, northwestern African Margin, (Leg 79, Deep Sea Drilling Project). *In* Hinz, K., Winterer, E. L., et al., *Init. Repts. DSDP*, 79: Washington (U.S. Govt. Printing Office), 497-508.

Chamley, H., Debrabant, P., Candillier, A.-M., and Foulon, J., 1983. Clay mineralogical and inorganic geochemical stratigraphy of Blake-Bahama Basin since the Callovian, Site 534, Deep Sea Drilling Project Leg 76. *In* Sheridan, R. E., Gradstein, F. M., et al., *Init Repts. DSDP*, 76: Washington (U.S. Govt. Printing Office), 437-451.

Debrabant, P., and Chamley, H., 1982. Influences océaniques et continentales dans les premiers dépôts de l'Atlantique Nord. *Bull. Soc. Geol. France*, 7, XXIV, 3:473-486.

Debrabant, P., and Foulon, J., 1979. Expression géochimique des variations du paléoenvironnement depuis le Jurassique supérieur sur les marges Nord-Atlantiques. *Oceanologica Acta*, 2, 4:469-475.

Deer, W. A., Howie, R. A., and Zussmann, J., 1963a. *Rock-Forming Minerals: Chain Silicates* (Vol. II): London (Longmans).

________, 1963b. *Rock-Forming Minerals: Sheet Silicates* (Vol. III): London (Longmans).

Desprairies, A., 1981. Authigenic minerals in volcanogenic sediments area during Deep Sea Drilling Project Leg 60. *In* Hussong, D. M., Uyeda, S., et al., *Init. Repts. DSDP*, 60: Washington (U.S. Govt. Printing Office), 455-466.

________, 1983a. Metamorphic processes in sediments in contact with young oceanic crust—East Pacific Rise, Leg 65. *In* Lewis, B. T. R., Robinson, P. T., et al., *Init. Repts. DSDP*, 65: Washington (U.S. Govt. Printing Office), 375-389.

________, 1983b. Relation entre le paramètre b des smectites et leur contenu en fer et en magnésium. Application à l'étude des sédiments. *Clay Minerals*, 18:165-175.

Desprairies, A., Bonnot-Courtois, C., Jehanno, C., Vernhet, S., and Joron, J.-L., 1984. Mineralogy and geochemistry of alteration products in Leg 81 basalts. *In* Roberts, D. G., Schnitker, D., et al., *Init. Repts. DSDP*, 81: Washington (U.S. Govt. Printing Office), 733-742.

Faure, G., 1978. Strontium abundance in common igneous rock types. *In* Wedepohl, K. H. (Ed.), *Handbook of Geochemistry* (Vol. II, 4): Berlin (Springer-Verlag).

Grim, R. E., and Kulbicki, G., 1961. Montmorillonite high-temperature reactions and classification. *Am. Mineral.*, 46:1329-1369.

Hoffert, M., 1980. Les "argiles rouges des grands fonds" dans le Pacifique centre—Est. Authigenèse, transport, diagenese. *Sciences Géologiques, Mém.*, 61.

Holtzapffel, T., Bonnot-Courtois, C., Chamley, H., and Clauer, N., 1985. Héritage et diagenèse dans la constitution des smectites Nord-Atlantiques (Crétacé-Paléogène). *Bull. Soc. Geol. France*, 1(8):25-33.

Holtzapffel, T., and Chamley, H., 1983. Morphologie et genèse de smectites albo-aptiennes et paléogènes de l'Atlantique Nord: héritage et recristallisation. *C. R. Acad. Sci.*, 296:1599-1602.

Lenôtre, N., Chamley, H., and Hoffert, M., in press. Nature and significance of Sites 576 and 578 clay stratigraphy (Leg 86 DSDP, Northwestern Pacific). *In* Heath, G. R., Burckle, L. H., et al., *Init. Repts. DSDP*, 86: Washington (U.S. Govt. Printing Office).

Mélières, F., Deroo, G., and Herbin, J.-P., 1981. Organic-rich and hypersiliceous Aptian sediments from western Mid-Pacific Mountains, Deep Sea Drilling Project Leg 62. *In* Thiede, J., Vallier, T. L., et al., *Init. Repts. DSDP*, 62: Washington (U.S. Govt. Printing Office), 903-921.

Millot, G., 1964. *Géologie des Argiles:* Paris (Masson).

Moberly, R., Schlanger, S. O., et al., 1983. The Mesozoic superocean. *Nature*, 302:381.

Stueber, A. M., 1978. Strontium abundance in rock-forming minerals; strontium minerals. *In* Wedepohl, K. H. (Ed.), *Handbook of Geochemistry* (Vol. II, 4): Berlin (Springer-Verlag).

Thiede, J., Dean, W. E., and Claypool, G. E., 1982. Oxygen-deficient depositional paleoenvironments in the mid-Cretaceous tropical and subtropical Pacific Ocean. *In* Schlanger, S. O., and Cita, M. B. (Eds.), *Nature and Origin of Cretaceous Carbon-Rich Facies:* London (Academic Press), pp. 79-100.

Weaver, C. E., and Beck, K. C., 1977. Miocene of the southeastern United Stages: a model for chemical sedimentation in a perimarine environment. *Sediment. Geol.*, 17# Spec. Issue.

Weaver, C. E., and Pollard, L. D., 1973. *The Chemistry of Clay Minerals:* Amsterdam (Elsevier).

Date of Initial Receipt: 11 May 1984
Date of Acceptance: 7 November 1984

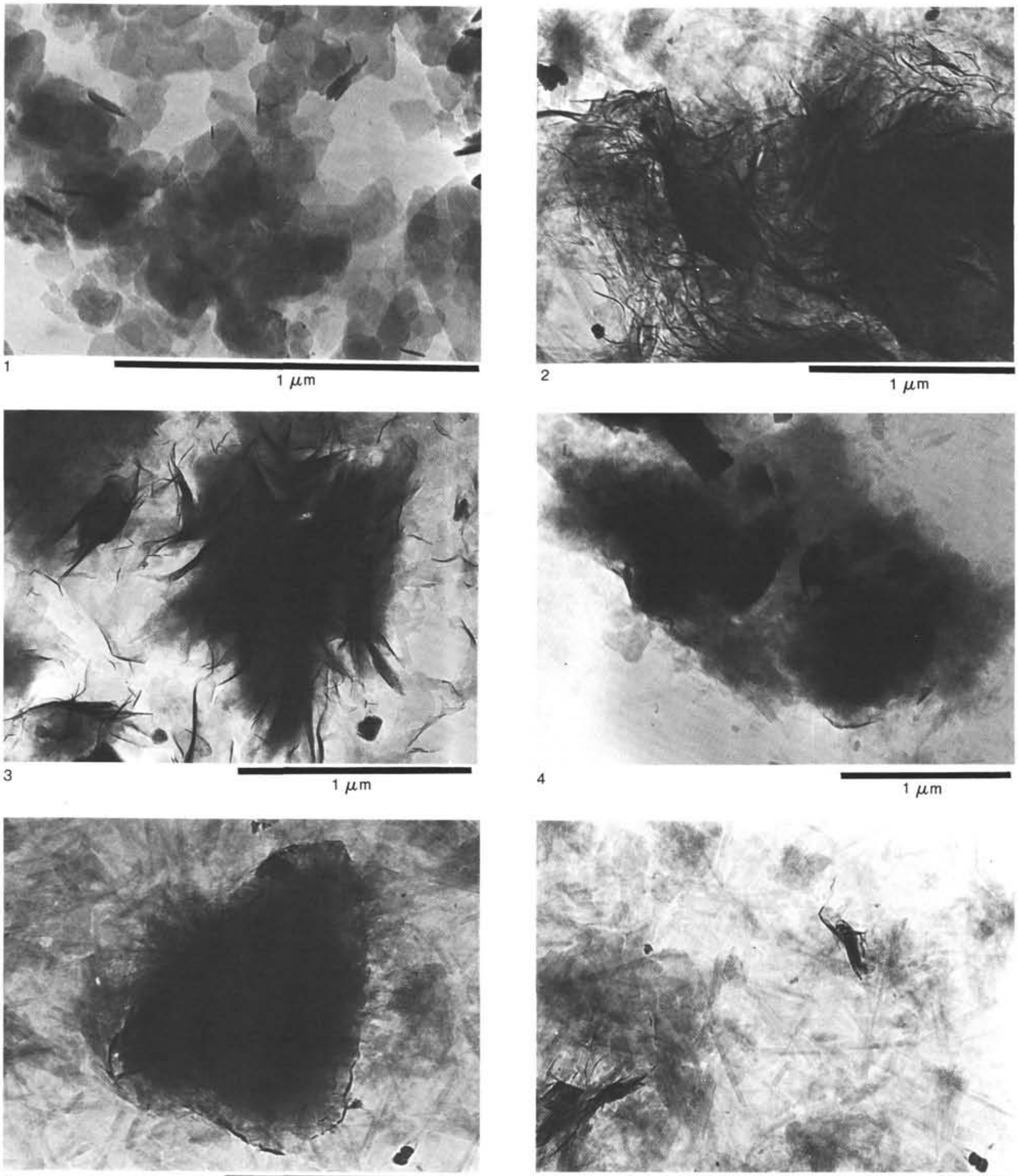

Plate 1. Micromorphologic types of smectites. **1.** Type 1: transparent smectites (Sample 585A-17-1, 15 cm, Zone 1, Aptian). **2.** Type 2: hairy smectites (Sample 585-44-3, 17 cm, Zone 2, Albian). **3.** Type 3: large folded smectites, probably indicative of a recurrent volcanic influence (Sample 585-26-1, 63 cm, Zone 3, Campanian). **4.** Type 4: fleecy smectites (Sample 585-46-2, 40 cm, Zone 2, Albian). **5.** Type 5: intermediate smectite with fleecy and lathed outlines (Sample 585-44-3, 17 cm, Zone 2, Albian; detail from Plate 3, Fig. 4). **6.** Type 6: isolated lathed smectites (Sample 585-44-3, 17 cm, Zone 2, Albian; detail from Plate 3, Fig. 4).

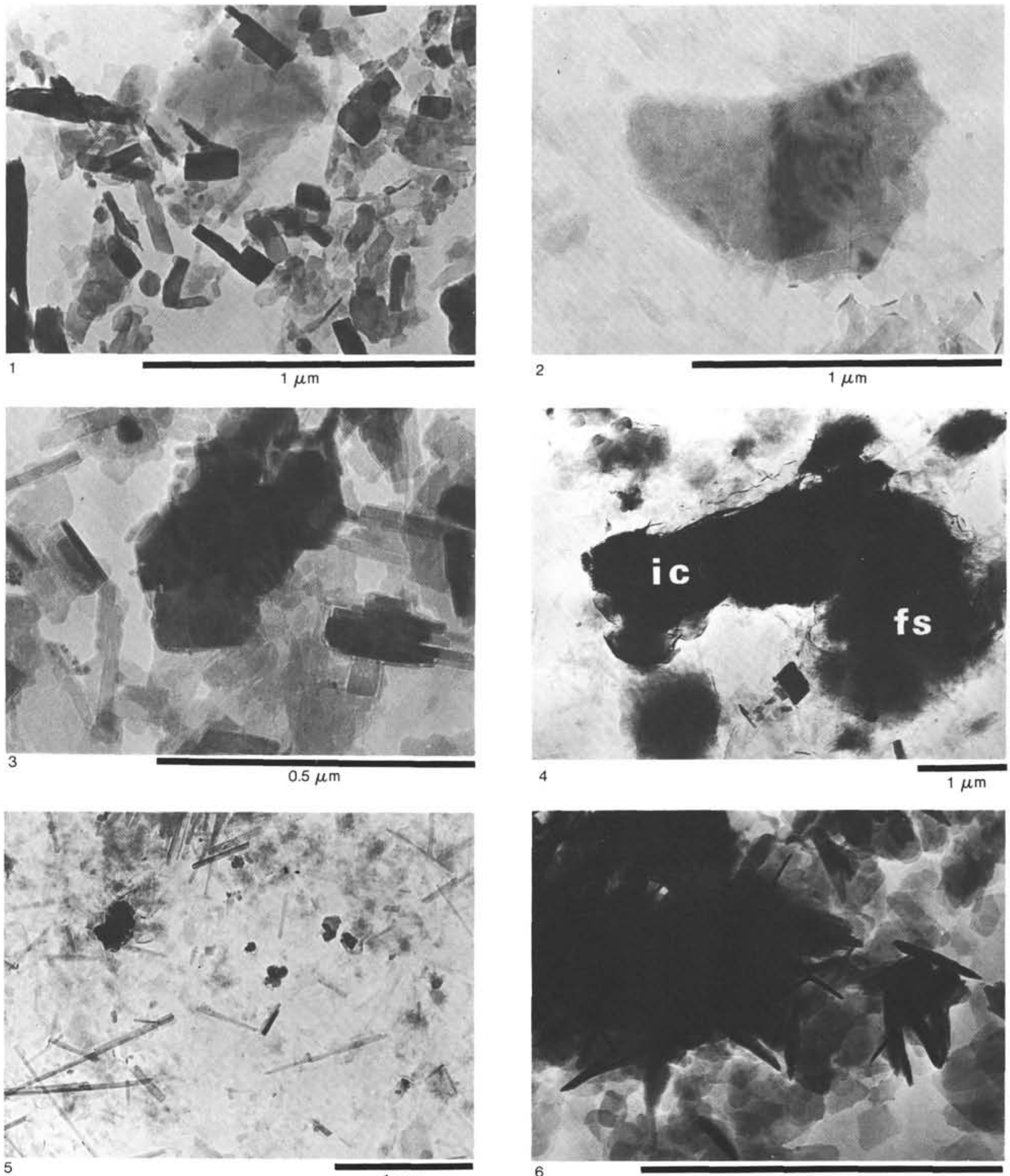

Plate 2. Other morphologic types. **1.** Illite, Type 1: small celadonite chips (Sample 585A-15-5, 137 cm, Zone 1, Aptian). **2.** Ilite, Type 2: typical micalike sheet (Sample 585-47-1, 9 cm, Zone 2, Albian). **3.** Chlorite, Type 1: hexagonal sheet (with celadonite chips) (Sample 585-48-2, 4 cm, Zone 2, Albian). **4.** Chlorite, Type 2: irregular dark and large sheet (ic) with fleecy smectite (fs) (Sample 585-46-2, 40 cm, Zone 2, Albian; detail from Plate 3, Fig. 2). **5.** Palygorskite fibers, more or less broken (Sample 585-34-2, 85 cm, Zone 3, Cenomanian). **6.** Small dark particles, with spiral shape, sometimes isolated, and sometimes constituting large aggregates (Al or Fe oxides?) (Sample 585A-17-1, 15 cm, Zone 2, Aptian).

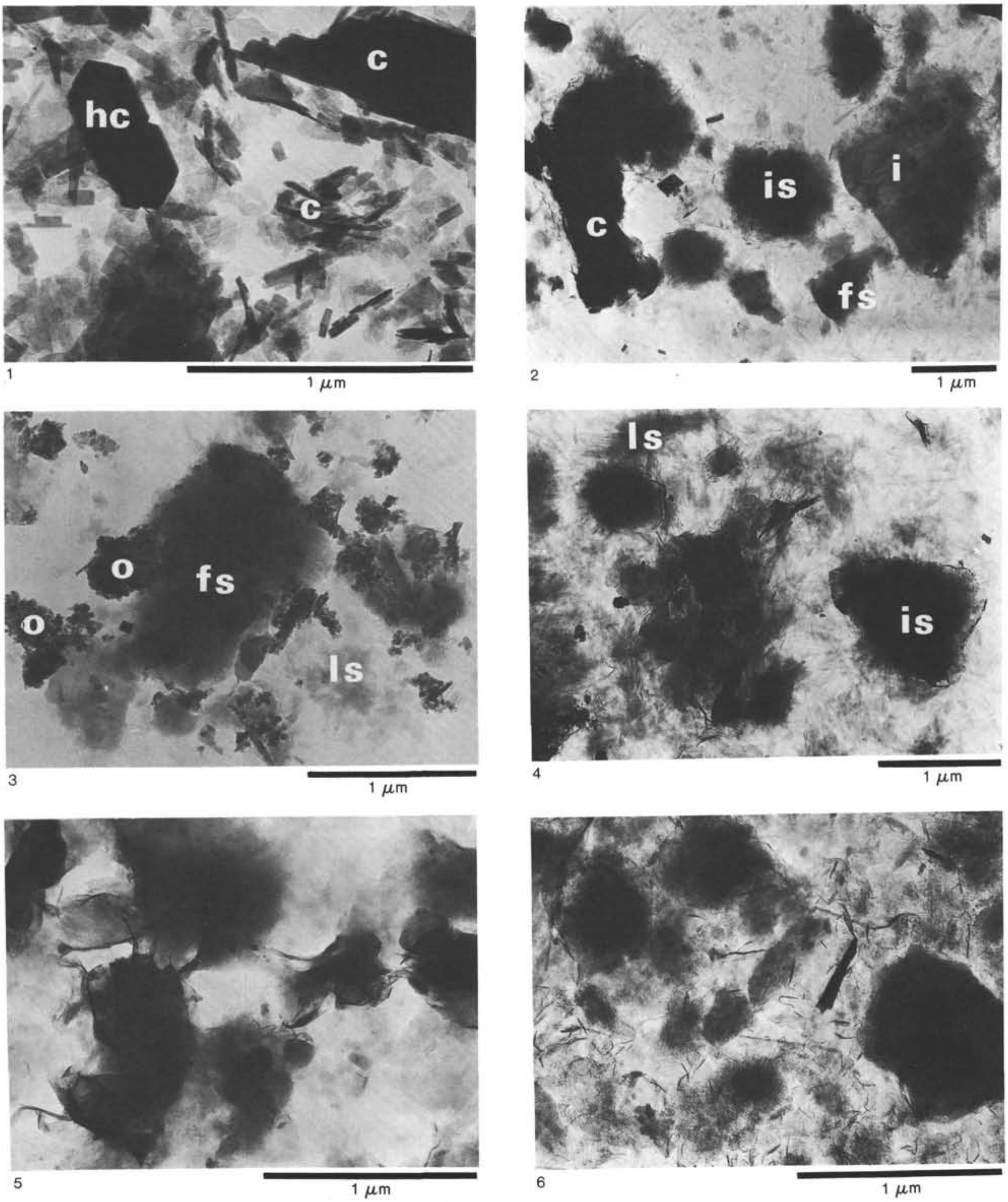

Plate 3. Examples of different morphologic clay assemblages. **1.** Zone 1 assemblage: transparent smectites, celadonite chips (c), and hexagonal chlorites (hc) (Sample 585-48-2, 4 cm, Zone 1, early Albian). **2.** Zone 2 assemblage: fleecy and intermediate smectites (fs; is), true illites (i), and irregular chlorite (c) (Sample 585-46-2, 40 cm, Zone 2, early Albian; see detail on Plate 2, Fig. 4). **3, 4.** Two assemblages with fleecy intermediate and lathed smectites (Zones 2 and 3). 3. Sample 585-27-4, 57 cm, Zone 3, Campanian: fleecy smectites (fs) are more abundant than intermediate ones (is); presence of opal (o). 4. Sample 585-44-3, 17 cm, Zone 2, Albian: lathed (ls) and intermediate smectites (is) are dominant. **5.** Peculiar assemblage of Zone 3 with folded smectites: recurrence of volcanic influence (Sample 585-27-1, 13 cm, Campanian). **6.** Zone 4, typical detrital assemblage: fleecy smectites, true illites, and rare palygorskite fibers (Sample 585-17-2, 146 cm, Maestrichtian).